



Cite this: *Nanoscale Adv.*, 2025, 7, 3846

## Hydroxycitrate-loaded exosomes demonstrate enhanced therapeutic efficacy against lung adenocarcinoma by inhibiting the metabolic enzyme ATP citrate lyase<sup>†</sup>

Kanika Phutela,<sup>a</sup> Amanjit Bal,<sup>b</sup> Navneet Singh<sup>c</sup> and Sadhna Sharma   <sup>ad</sup>

Cancer cells display the Warburg effect resulting in the production of excess pyruvate that is converted to acetyl-CoA in the mitochondria. Acetyl-CoA is further converted to citrate in the mitochondria. Meanwhile, in the cytosol, citrate is cleaved by ATP citrate lyase (ACLY) that regenerates acetyl-CoA and oxaloacetate. Recently, ACLY has been recognized as a potential target owing to its overexpression in several cancers, including non-small cell lung cancer. The aim of this study was to develop an ACLY-targeting exoformulation, where bovine milk-derived exosomes were surface-conjugated with folate and loaded with the natural ACLY inhibitor potassium hydroxycitrate. The therapeutic efficacy of potassium hydroxycitrate was enhanced by encapsulating it in bovine milk exosomes, and the anti-cancer potential of this exoformulation was evaluated in urethane-induced lung adenocarcinoma murine model. Potassium hydroxycitrate-loaded exosomes, which were surface-conjugated with folate (Exo-KH), exhibited a particle size of ~183 nm and a practical loading efficiency of ~16.8%. The exoformulation was found to be spherical in shape as characterized by scanning electron microscopy. Pharmacokinetic studies confirmed the continuous release of hydroxycitrate from the exoformulation, and Exo-KH administered mice showed inhibition of lung tumor growth. The mRNA expression levels of ACLY and other metabolic enzymes, such as FASN, HMGCR, SERBP1c, were also reduced in the exoformulation-treated group as compared with its free form-treated group. ACLY activity was also observed to be decreased in serum and tumor lysates of exoformulation-treated mice. This study demonstrates the potential of using bovine milk exosomes encapsulating potassium hydroxycitrate as a new chemotherapeutic option for non-small cell lung cancer.

Received 27th January 2025  
Accepted 28th April 2025

DOI: 10.1039/d5na00094g  
[rsc.li/nanoscale-advances](http://rsc.li/nanoscale-advances)

## Introduction

Lung cancer is one of the deadliest diseases worldwide with highest mortality rates among both men and women.<sup>1</sup> Majority of the people are diagnosed with lung cancer at an advanced stage (II or IV), which makes it difficult to cure, and radiation therapy and chemotherapy are the only treatment options available in such cases.<sup>2</sup> Adenocarcinoma accounts for 40% of lung cancer cases, and these tumours tend to grow on the lung

periphery and can metastasize to other body tissues.<sup>3</sup> Cancer cells commonly use glycolysis as their only method for energy production.<sup>4</sup> Excess pyruvate produced because of enhanced aerobic glycolysis is excreted out of the cell as lactate; however, pyruvate also undergoes conversion to acetyl-CoA in mitochondria. Owing to the increase in citrate levels, it is exported to cytosol, where it gets converted to acetyl-CoA and oxaloacetate by ATP citrate lyase (ACLY).<sup>5</sup> Acetyl-CoA contributes to fatty acids synthesis, cholesterol biosynthesis and histone acetylation. Currently, ACLY is being explored for treatment of pathological conditions such as cancer. It has been reported that ACLY expression is constantly increased in several cancers including bladder, stomach, lung, breast, and liver tumors.<sup>6–9</sup>

Hydroxycitrate is a competitive inhibitor of the metabolic enzyme ACLY. It is an active ingredient of the plant *Garcinia cambogia*, which are grown in parts of the Indian sub-continent, and it is also present in various dietary supplements.<sup>10</sup> It has been reported that hydroxycitrate is not only useful for the treatment of metabolic diseases but also has antitumor activity.<sup>11,12</sup> Notably, ACLY activity declined to 86.6% in

<sup>a</sup>Department of Biochemistry, Postgraduate Institute of Medical Education and Research, Chandigarh, India

<sup>b</sup>Department of Histopathology, Postgraduate Institute of Medical Education and Research, Chandigarh, India

<sup>c</sup>Department of Pulmonary Medicine, Postgraduate Institute of Medical Education and Research, Chandigarh, India

<sup>d</sup>Department of Biochemistry, Postgraduate Institute of Medical Education and Research, PGIMER, MAMS, FACB, FIABS, Chandigarh, India. E-mail: [sadhna.biochem@gmail.com](mailto:sadhna.biochem@gmail.com)

<sup>†</sup> Electronic supplementary information (ESI) available. See DOI: <https://doi.org/10.1039/d5na00094g>



colonocytes after treatment with 7 mM HCA.<sup>13</sup> Calcium hydroxycitrate also inhibited the invasion and enhanced the activity of HMG-CoA reductase in HepG2 cells.<sup>14</sup> However, it was found that the bioavailability of hydroxycitrate is low, and a specialized delivery system is required for its efficient application for lung cancer treatment. In this regard, nanomaterials (1–100 nm) are frequently utilized at different stages of nanomedicine<sup>15–17</sup> due to their ability to circulate in the body for longer duration, thereby reducing toxicity and the need for frequent medications.<sup>18</sup> Bovine milk exosomes possess some unique characteristic features such as biocompatibility, endogenous origin, and targeted drug delivery which together make them potential drug delivery vehicles. Moreover, bovine milk is easily available, economical, and has important nutritional benefits.<sup>19</sup> Bovine milk exosomes have been used to deliver different types of therapeutic compounds (paclitaxel, doxorubicin, warfarin, and curcumin) to the recipient cells without exerting any toxicity and immunogenicity.<sup>20–22</sup> Curcumin and other unstable molecules such as paclitaxel can exhibit improved therapeutic effects after being loaded in bovine milk exosomes. Different curcumin delivery vehicles (ferritin and liposomes) have been previously employed to improve curcumin's solubility but synthetic delivery vehicles have specific drawbacks such as activation of a complement system and circulating antibodies that can decrease the efficiency of synthetic carriers.<sup>23</sup> On the other hand, curcumin loaded in bovine milk exosomes was found to resist gastrointestinal digestion and these exosomes could easily transfer their contents across the intestinal barrier into the blood circulation.<sup>24</sup> Another widely used anti-cancer drug with low bioavailability is paclitaxel, and its nanoparticle-based formulation (Abraxane®, albumin-bound nano-formulation) is being used clinically; however, a significant decrease in white and red blood cells, and allergic reactions have been observed upon its intravenous administration.<sup>25</sup> These adverse immunological effects were overcome through the oral administration of bovine milk exosomes loaded with paclitaxel (EXO-PAC) and significant tumor growth inhibition was observed, thereby reducing the complications associated with intravenous usage of this drug.<sup>26</sup>

The targeting ability of these exosomal formulations can be further enhanced using ligands such as folate. Folate conjugates can enter cancer cells *via* receptor-mediated endocytosis. Therefore, folate receptor is a popular ligand that is commonly used in various drug delivery systems targeting FR-positive tumors.<sup>27</sup> The development of novel drug delivery systems targeting FRs can potentially decrease the nonspecific distribution of chemotherapeutic drugs. Therefore, the present work is focused at determining the therapeutic efficacy of bovine milk exosomes encapsulating the potassium hydroxycitrate surface-conjugated with folate for lung adenocarcinoma treatment.

## Materials and methods

### Animals

Inbred Balb/c male mice (20–25 g body weight, 8–10 weeks old) were obtained from the Institutional Advanced Animal Facility of PGIMER, Chandigarh. All animal experiments were conducted by strictly adhering to the guidelines of the Committee

for the Purpose of Control and Supervision of Experiments on Animals (CPCSEA). The study was ethically approved by the Institutional Animal Ethics Committee (ref no: 100/IAEC/702) of PGIMER, Chandigarh. The animals were kept in ethically approved conditions (12-hour day/night cycle) and food and water were given ad libitum.

### Isolation of exosomes

Milk was procured from a local farm and exosome isolation was done by differential centrifugation as described previously.<sup>28</sup> In brief, milk was centrifuged at 10 000×*g* for 30 min to remove the fat layer followed by centrifugation at 100 000×*g* for 60 min and the supernatant was then centrifuged at 135 000×*g* for 90 min to pellet the exosomes. The exosome pellet was subjected to PBS washing and filtered through 0.22 µm filter to remove any residual large particles. The exosome protein concentration was adjusted to 3–4 mg mL<sup>−1</sup> and aliquots were kept at −80 °C for further use.

### Preparation of potassium hydroxycitrate-loaded exosomes

The exosome suspension (5 mg) was mixed with potassium hydroxycitrate (10 mg) in the proportion of 1 : 2, and this mixture was subjected to six cycles of sonication (30 s each, 20% amplitude) and then the Exo-KH mixture was kept at 37 °C for 60 min.<sup>21</sup> For folate conjugation, 1 mg of activated folate was added to the exosome drug mixture and incubated at 22 °C for 30 min. The folate-NHS conjugate was prepared as previously described.<sup>29</sup> The Exo-KH solution was centrifuged at 10 000×*g* for 15 min and supernatant was centrifuged at 150 000×*g* for 90 min. The Exo-KH pellet obtained was dissolved in 1× PBS and stored at −80 °C.

### Characterization of exosomal formulation

The exosomes and Exo-KH were characterized for their particle size by dynamic light scattering (DLS) and their surface morphology analysis was performed by scanning electron microscopy (SEM) at 20 kV. The presence of the vital exosomal surface protein Alix was analysed by western blotting (Cell-Signaling, Danvers, MA). Folate conjugation on the exosome surface was estimated by measuring the absorption at 370 nm. The amount of potassium hydroxycitrate was quantified in exosomes using UHPLC (Thermo Fisher, USA). Potassium hydroxycitrate was estimated using double distilled filtered water as the mobile phase in a C18 column at flow rate of 1 m min<sup>−1</sup> at 30 °C, and the absorbance was measured at 210 nm. Drug loading capacity was quantified as the amount of drug (mg) entrapped per mg of the formulation developed. The percentage drug entrapment efficiency was calculated as: [amount of drug (mg) encapsulated in exosomes]/[amount of drug (mg) initially taken] × 100.

### In vitro release study

For determining the drug release profile, 0.1% Tween 80 was added to PBS (pH 7.4) containing the exoformulation and this medium was kept at 37 °C with continuous stirring at 100 rpm.



Aliquots of 1 mL were withdrawn at different time intervals (0.5, 1, 2, 4, 8, 16, 24, 36, and 48 h) and replaced with an equal volume of PBS after each sampling. The concentration of potassium hydroxycitrate was determined by HPLC as mentioned above.

### Pharmacokinetic studies

Male Balb/c mice (25–30 g) were maintained in the institutional animal facility and kept on a 12 h day per night cycle. Potassium hydroxycitrate was administered at a dose of 250 mg kg<sup>-1</sup> and mice were randomly categorized into different groups with 12 mice in each group: Group I mice were administered free potassium hydroxycitrate orally, Group II animals were administered free potassium hydroxycitrate intraperitoneally and Group III mice were administered exosome loaded potassium hydroxycitrate intraperitoneally. Blood withdrawal was performed from the jugular vein at 0.5, 1, 2, 4, 8, 16, 24, 48 and 72 h from 4–5 animals/time point. The blood was centrifuged at 3000 rpm for 10 min to separate the serum. Potassium hydroxycitrate levels were estimated in various tissues such as liver, lung, kidney, spleen, and heart. The tissue homogenates were prepared by homogenizing the tissue samples in PBS using a homogenizer and then centrifuged at 20 000×g for 20 min at 4 °C. The clear supernatant was used to determine the concentration of potassium hydroxycitrate as mentioned in the ESI.† Pharmacokinetic parameters were estimated using R and WinNonlin software.

### Urethane-induced lung cancer murine model development

Inbred male balb/c mice (8–10 weeks, 25–30 kg body wt) were used for the development of lung adenocarcinoma model. Mice were administered intraperitoneally with three doses of urethane (1 g kg<sup>-1</sup>) in saline with a gap of 15 days.<sup>30</sup> The development of the tumor lesions was tracked by sacrificing the urethane treated mice at 8, 16, 24 and 40 weeks by histopathological analysis. The tumors were confirmed to be adenocarcinoma by immunohistochemistry for the lung adenocarcinoma marker TTF-1 as mentioned in the ESI† (Cell Marque, USA).

### Therapeutic efficacy studies

Male balb/c mice which were treated with urethane were used for evaluating the therapeutic efficacy of free and exosome loaded potassium hydroxycitrate after a 40 weeks latency period. Free and exoformulated potassium hydroxycitrate was administered intraperitoneally 250 mg per kg b. wt once a day for 2 weeks continuously and the control group was administered saline every day (six mice/group). Another group of mice was administered exosomes alone intraperitoneally. The weight of the animals was monitored on alternate days and the mice were sacrificed after the completion of 30 days, with the lungs and other tissues removed. The tumor volume was calculated by measuring the tumor size using a Vernier calliper.<sup>31</sup>

### Gene expression analysis

The tumor lesions were used for RNA isolation and 1 µg of total RNA was converted to single stranded cDNA. Briefly, 1 mL of Trizol reagent was added to lyse the cells, followed by the addition of 0.2 mL of chloroform and centrifuged at 12 000×g for 15 min at 4 °C. Then, 0.5 mL of 100% isopropanol was added to the aqueous phase and centrifuged at 12 000×g for 10 min at 4 °C to precipitate the RNA. The pellet was first incubated at 55–60 °C in a dry bath for 15 min and then resuspended in 20 µL of RNase free water and stored at –80 °C for further analysis.<sup>32</sup> The gene expression of ATP citrate lyase and other lipogenic enzymes, along with apoptosis and autophagy markers, was analyzed in treated and untreated groups. Beta-actin was used as the housekeeping gene.<sup>33</sup> The primer sequences of different genes are given in Table 1.

### ATP citrate lyase activity assay

Cell lysates were prepared from the lung tumor lesions of treated and untreated mice in 200 µL of RIPA buffer with protease inhibitor cocktail. The sample (100 µL) was added at a 1:9 ratio to the reaction mixture containing 100 mM Tris-HCl (pH 8.7), 20 mM potassium citrate, 10 mM MgCl<sub>2</sub>, 10 mM DTT, 0.5 U mL<sup>-1</sup> malate

Table 1 Primer sequences

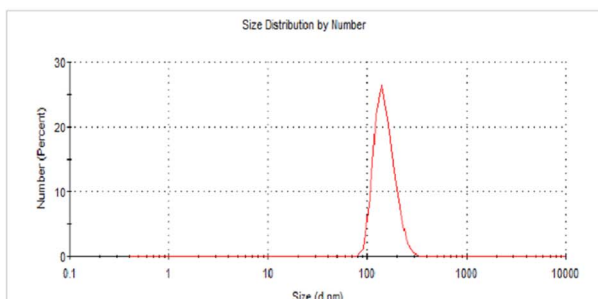
Gene	Forward primer	Reverse primer
Beta-actin (ACTB)	CATTGCTGACAGGATGCAGAA	TGCTGGAAGGTGGACAGTGAG
Epidermal growth factor receptor (EGFR)	CAGCTTACGTACTGATACGC	GTCCAATACGTAACCGGATG
Folate receptor alpha (FR α)	TGGTCGTGAAATTGTCCT	GGACTGAACCTCTCAATGTC
ATP citrate lyase (ACLY)	TGAAGAAGGAGGGGAAGCTG	AGTCCTGAGCATGTCCACA
Fatty acid synthase (FASN)	CCGTCGTTATACCACTGCT	GGCAAAGCTGGTGTCAAA
Acetyl CoA carboxylase (ACC)	TCTGGCCTCCACTTTGCTA	TACCATCACACTGCCATGT
HMG CoA reductase (HMGCR)	GAGATCATGTGCTGCTTCGG	CTTGGGTTACGGGTTGG
Citrate synthase (CS)	GTAGCTCTCCCTTCGGTC	CCATGTTGCTGTTGAAGGT
Isocitrate dehydrogenase I (ICD1)	TGGCACCATCCGAAACATTC	CTACTTTCCAGGCCAGGA
B-cell lymphoma 2 (Bcl-2)	AGCCAAGCAGACGTAGAAGT	AACTGTGGCTCTCATGGACA
Bcl-2 associated X-protein (Bax)	GGATGATTGCTGACGTGGAC	ATGGTTCTGATCAGCTCGGG
Caspase 3	CGAAAGAAACAGATCCGT	TCGAAGTTGAGGTAGCTGCA
Autophagy related 5 (Atg5)	GAAGAGGAGGCCAGGTGATGA	GTGGTTCCATCTAGCGAGGA
Beclin-1	AGCTGGAGTTGGATGACGAA	CCCAGGCAGCATTGATTCA
Microtubule-associated protein 1A/1B-light chain 3 (LC3B)	CCCATCTCCGAAGTGTACGA	GGGTGCTACGTTCTCATCT
Sterol regulatory element-binding protein-1C (SREBP-1C)	GTCAAACACCAGCCTCCAAAG	GTCCCCGTCCACAAAGAAAC



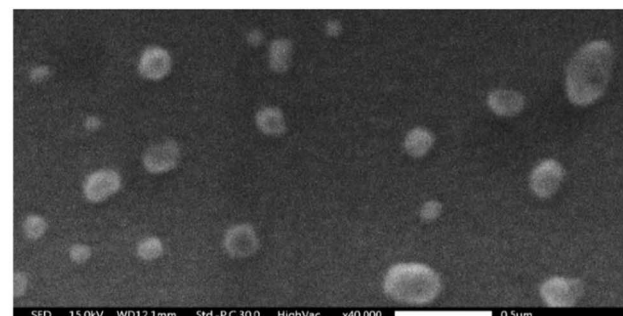
dehydrogenase, 0.14 mM NADH, 0.33 mM CoA (added at last) and 5 mM ATP. Change in absorbance was measured at 340 nm and absorbance per minute was calculated.<sup>6</sup>

### Statistical analysis

Statistical tests, such as Mann–Whitney, Kruskal–Wallis and one-way ANOVA tests, were performed using SPSS and



(a)

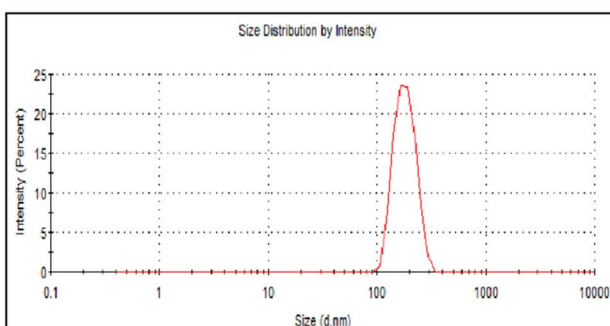


(b)

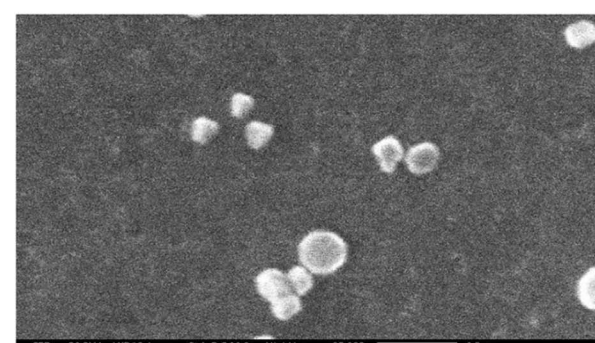
Exo Lysate

Alix  
(90-100Kda)

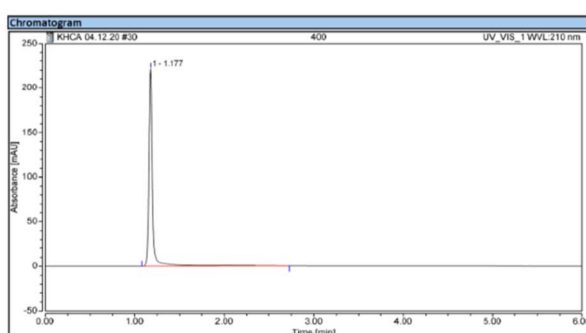
(c)



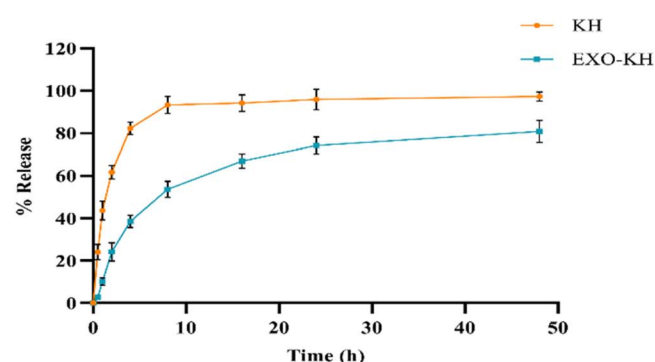
(d)



(e)



(f)



(g)

**Fig. 1** Characterization of bovine milk exosomes with respect to (a) size distribution of exosome suspension (diluted 10-fold in 1× PBS, pH 7.4) using dynamic light scattering, (b) surface morphology using scanning electron microscopy, (c) surface markers using western blotting analysis, (d) size distribution of potassium hydroxycitrate exosomes, (e) scanning electron microscopy image of exoformulation, (f) HPLC chromatogram of potassium hydroxycitrate (detailed conditions of HPLC conditions are given in the materials and methods section) and (g) release profile of KH evaluated from the exoformulation. Values are presented as mean  $\pm$  SD of three independent formulations.

GraphPad software. Pharmacokinetic analysis was done by non-compartmental analysis using R package (version 0.9.4). The R analysis was verified by WinNonlin Software.

## Results

### Preparation and characterization of potassium hydroxycitrate encapsulating exosomes

Bovine milk was used for exosome isolation by ultracentrifugation. The average yield of the exosomes was  $153.4 \pm 16$  mg per litre of milk. The size of the exosomes and hydroxycitrate exoformulation was  $96.23 \pm 16.82$  nm and  $183 \pm 21.3$  nm respectively as measured by the dynamic light scattering (DLS) technique (Fig. 1a and d). The polydispersity index and zeta potential of the exoformulation was  $0.28 \pm 0.03$  and  $-14.35 \pm 1.78$  mV calculated at  $37^\circ\text{C}$  using a zetasizer. The exosome and exoformulation were spherical in morphology and their size was confirmed to be  $<200$  nm by scanning electron microscopy (SEM) (Fig. 1b and e). The exosome protein lysates showed positivity for the vital exosomal membrane marker ALIX (Fig. 1c). ALIX (ALG-2-interacting protein X) is a cytoplasmic protein ubiquitously expressed in exosomes. It is associated with the endosomal sorting complex required for transport (ESCRT) and sorting of cargo into the exosomes; thus, it is commonly used as a marker for exosomes.<sup>29</sup> The amount of folate conjugated to exosomes was in the range of  $40.10\% \pm 4.86\%$ . The encapsulation efficiency of hydroxycitrate was found to be  $16.87\% \pm 2.78\%$  and drug loading capacity was  $10.23\% \pm 1.28\%$  as estimated after solvent extraction of the drug followed by UHPLC analysis (Fig. 1f). Also, the *in vitro* release profile of KH from the exosomes under physiological conditions showed a sustained drug release pattern over a period of 48 h (Fig. 1g).

### Pharmacokinetic studies of free and exoformulation of potassium hydroxycitrate

The pharmacokinetic profile of free and potassium hydroxycitrate encapsulating exosomes was studied in male Balb/c mice. The pharmacokinetic profile of free KH when administered orally or intraperitoneally revealed its presence in the serum for a comparatively shorter duration than its exoformulation (EKH) as observed from the early  $T_{1/2}$  and  $k_e$  values (Table 2). Free hydroxycitrate was detected in the liver and lung tissue for up to

48 h (Fig. 2a and b) and Exo-KH also showed similar tissue distribution pattern when administered intraperitoneally (Fig. 2c).

Exo-KH had a higher area under curve in the plasma drug concentration *versus* time curve compared with free KH (Fig. S1†). The plasma area under the curve (AUC) value for the exoformulation (Exo-KH) was approximately 5-fold higher than that for free potassium hydroxycitrate. The pharmacokinetic study depicted the extended retention and continuous release of hydroxycitrate from the exoformulation in the systemic circulation.

### Therapeutic efficacy of free and exosome loaded hydroxycitrate against lung adenocarcinoma

The urethane treated mice were able to develop lung tumor lesions after 2 months of treatment and were observed until 10 months for the development of fully formed lung tumors (Fig. 3a-d) that represented the advanced disease stage and were further confirmed by TTF-1 nuclear positivity (Fig. 3e-g). Based on these results, the anti-tumor efficacy study was conducted in the 10-month latency period. The therapeutic efficacy of free and exoformulated potassium hydroxycitrate was tested in lung tumor bearing mice. The dose frequency was based on the pharmacokinetic parameters.

### Survival analysis and tumor burden estimation

After completion of the treatment regimen, the animals were monitored for 30 days, and survival outcomes were drawn (Fig. 4A(a)). The tumor volume decreased in both FKH and EKH treated groups (Fig. 4A(b)). In the exosome alone and untreated groups, seven-eight tumors were seen (Fig. 4A(c) and B(a and d)) whereas in the free and EKH groups, the average tumor number was reduced to three and two, respectively (Fig. 4A(c) and B(b and c)). The tumor cells present in the tumor nodules were organized in a glandular pattern, representing ideal characteristic features of adenocarcinoma (Fig. 4C(a and b)). The tumor nodules had few apoptotic areas along with lymphocytic infiltration in both the treated groups (Fig. 4C(c and d)). In addition to the lung tissue, other vital organs such as the liver and kidney were examined for histological changes (Fig. S2†).

**Table 2** Pharmacokinetic parameters based on serum levels of free potassium hydroxycitrate administered orally and intraperitoneally and exoformulated potassium hydroxycitrate administered intraperitoneally<sup>a</sup>

Pharmacokinetic parameters for serum						
Drug	Maximum serum drug concentration $C_{\max}$ ( $\mu\text{g mL}^{-1}$ )	Half-life $T_{1/2}$ (h)	Time of peak drug concentration $T_{\max}$ (h)	Clearance ( $\text{mg L}^{-1}$ )	Area under the curve AUC ( $\mu\text{g h mL}^{-1}$ )	Drug elimination rate constant $k_e$ ( $\text{mL h}^{-1}$ )
Free KH oral	$239.63 \pm 28.43$	$6.00 \pm 0.163$	1.5	$1.03 \pm 0.32$	$812.05 \pm 142.48$	$0.115 \pm 0.003$
Free KH IP	$360.38 \pm 57.25$	$7.98 \pm 0.258$	8	$2.67 \pm 0.41$	$10\ 040.16 \pm 1655.87$	$0.087 \pm 0.003$
EXO-KH IP	$2087.70 \pm 680.80$	$153.55 \pm 37.32$	24	$0.133 \pm 0.07$	$47\ 839.33 \pm 11\ 973.38$	$0.032 \pm 0.001$

<sup>a</sup> Values are represented as means  $\pm$  SD of 4–5 animals at each time point.



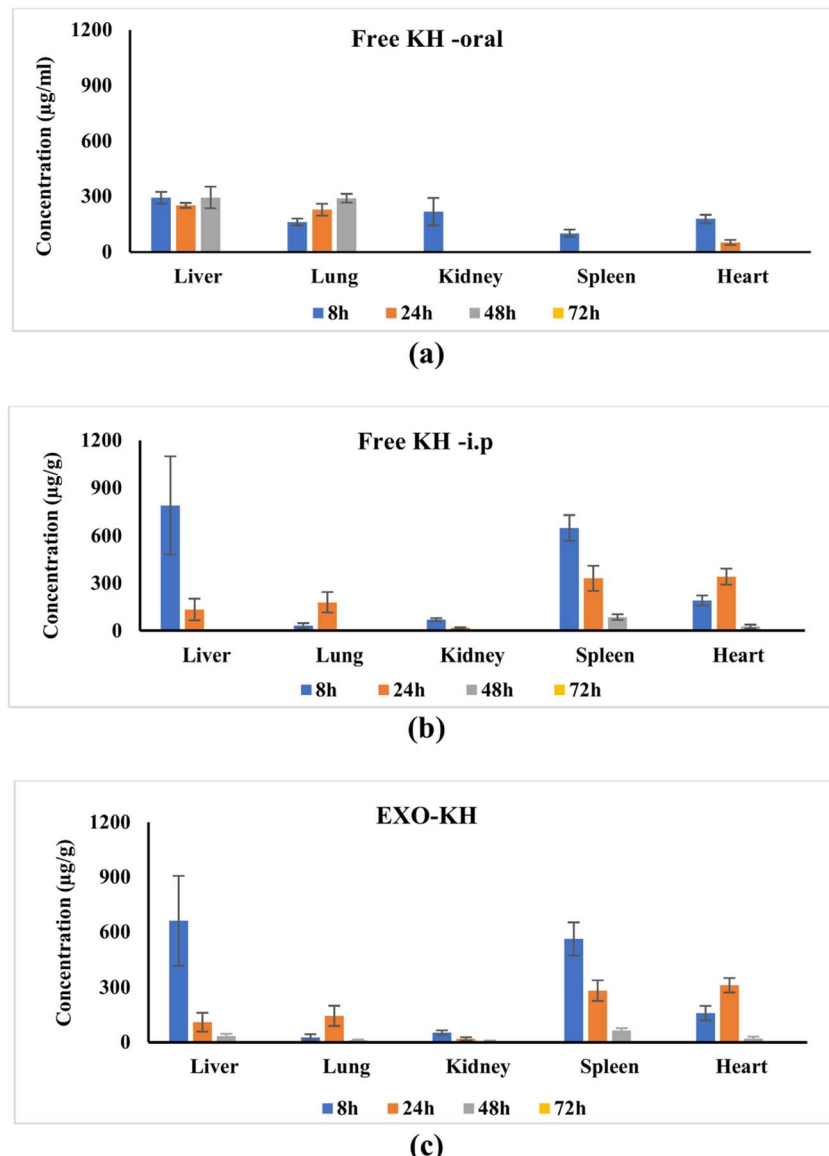
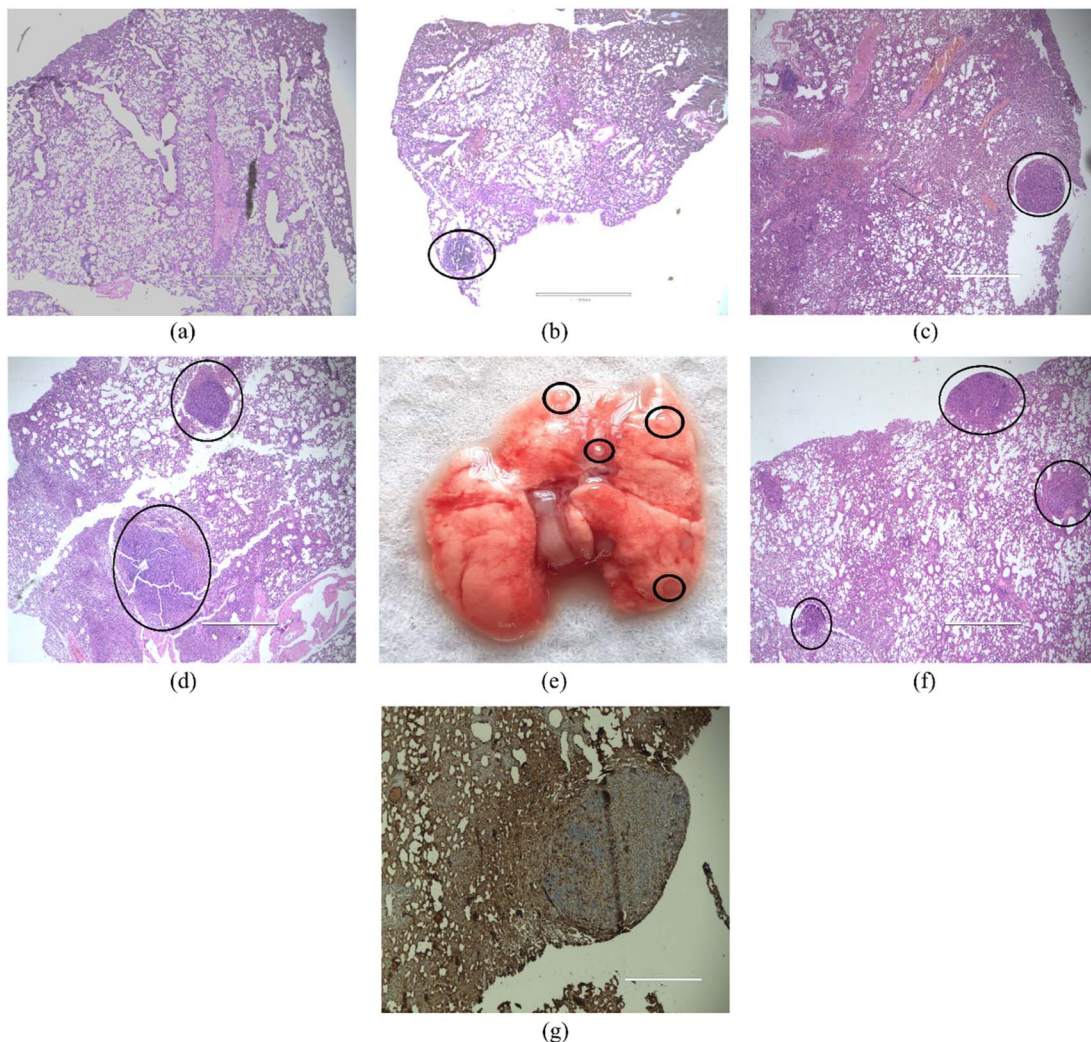


Fig. 2 Drug levels in various organs after administration of a single dose of (a) free potassium hydroxycitrate administered orally (b) free potassium hydroxycitrate administered intraperitoneally and (c) exoformulated potassium hydroxycitrate administered intraperitoneally. Values are presented as mean  $\pm$  SD of 4–5 animals at each time point.

### Gene expression analysis of the tumor lesions

Both free potassium hydroxycitrate and exoformulation-treated groups showed decreases in EGFR and folate receptor  $\alpha$  expression compared with the untreated group (Fig. 5a and b). The changes occurring at the gene level were determined to assess the therapeutic efficacy of this treatment regimen and establish a correlation with tumor load and survival rate. The EKH group showed a significant decrease in ACLY expression compared with its free form treated group (Fig. 5c). The expression of FASN was decreased in the exoformulation group while the free drug group showed upregulation of FASN expression (Fig. 5d). The expression of acetyl CoA carboxylase and HMG-CoA reductase significantly decreased in free and exoformulation of potassium hydroxycitrate groups compared

with the untreated group (Fig. 5e and f). Free and exoformulated potassium hydroxycitrate groups showed upregulation of citrate synthase expression (Fig. 5g) while the expression of isocitrate dehydrogenase 1 was decreased in both the free and exoformulation groups (Fig. 5h). Sterol element regulatory binding protein, a major transcription factor that controls fatty acid synthesis and lipogenesis decreased in the exoformulation group (Fig. 5i). The expression of Protein kinase B (also known as AKT, which directly activates ACLY by phosphorylating it) was decreased in both free and exoformulated potassium hydroxycitrate groups (Fig. 5j). The gene expression of apoptosis and autophagy related markers was evaluated to determine the cytotoxic effects of this treatment regimen. Bcl-2, an apoptosis suppressor gene, decreased in both free potassium hydroxycitrate and exoformulated groups (Fig. 6Aa). The expression of



**Fig. 3** Lung adenocarcinoma model development. Illustrative lung images of (a) control, (b) H&E tumor images at 2 months, (c) 4 months, (d) 6 months and (f) 10 months. (e) Gross tumor lesion at 10 months. (g) TTF-1<sup>+</sup> tumor lesion at 10 months of latency. Black circles highlight the lung tumor lesions.

Bax (an apoptosis activator gene) decreased in the EKH treated group while there was no change in the free potassium hydroxycitrate group (Fig. 6A(b)). Caspase-3 is involved in the final steps of apoptosis. Its expression increased in the EKH group compared with its free form treated and untreated groups (Fig. 6A(c)). LC3B is an important marker of autophagy, and its expression was observed to be downregulated in both the free form and EKH group compared with the untreated group (Fig. 6A(d)). Likewise, ATG5 expression decreased in both the free and EKH groups whereas Beclin-1 expression was upregulated in both groups (Fig. 6A(e and f)).

#### Estimation of ACLY activity in tumor lesions

After the completion of the therapy period, blood samples were withdrawn, and the lung tumor nodules were excised from all the study groups. In the exoformulation group and its free form group, a significant decrease in ACLY activity was observed in serum samples (Fig. 6B(a)). A similar trend was observed in

tumor tissue samples where ACLY activity was substantially downregulated in both free and exoformulation-treated groups (Fig. 6B(b)).

## Discussion

Cancer cells display tremendous increase in their proliferation potential due to the alterations in metabolic pathways. They exhibit increased *de novo* lipid synthesis by elevation in fatty acid synthesis and mevalonate pathway, providing the necessary macromolecules to meet the increased energy demands. A few years ago, ATP citrate lyase (ACLY) emerged as an attractive target for cancer treatment. In the cytosol, ACLY converts citrate into acetyl-CoA and oxaloacetate. Hydroxycitrate is one of the natural inhibitors of ACLY and has been used in a few studies along with some already approved anticancer agents where it showed potential anticancer effects.<sup>12</sup> However, potent drug delivery vehicles are required for its efficient transport to cancer cells because of its low bioavailability.<sup>11</sup>



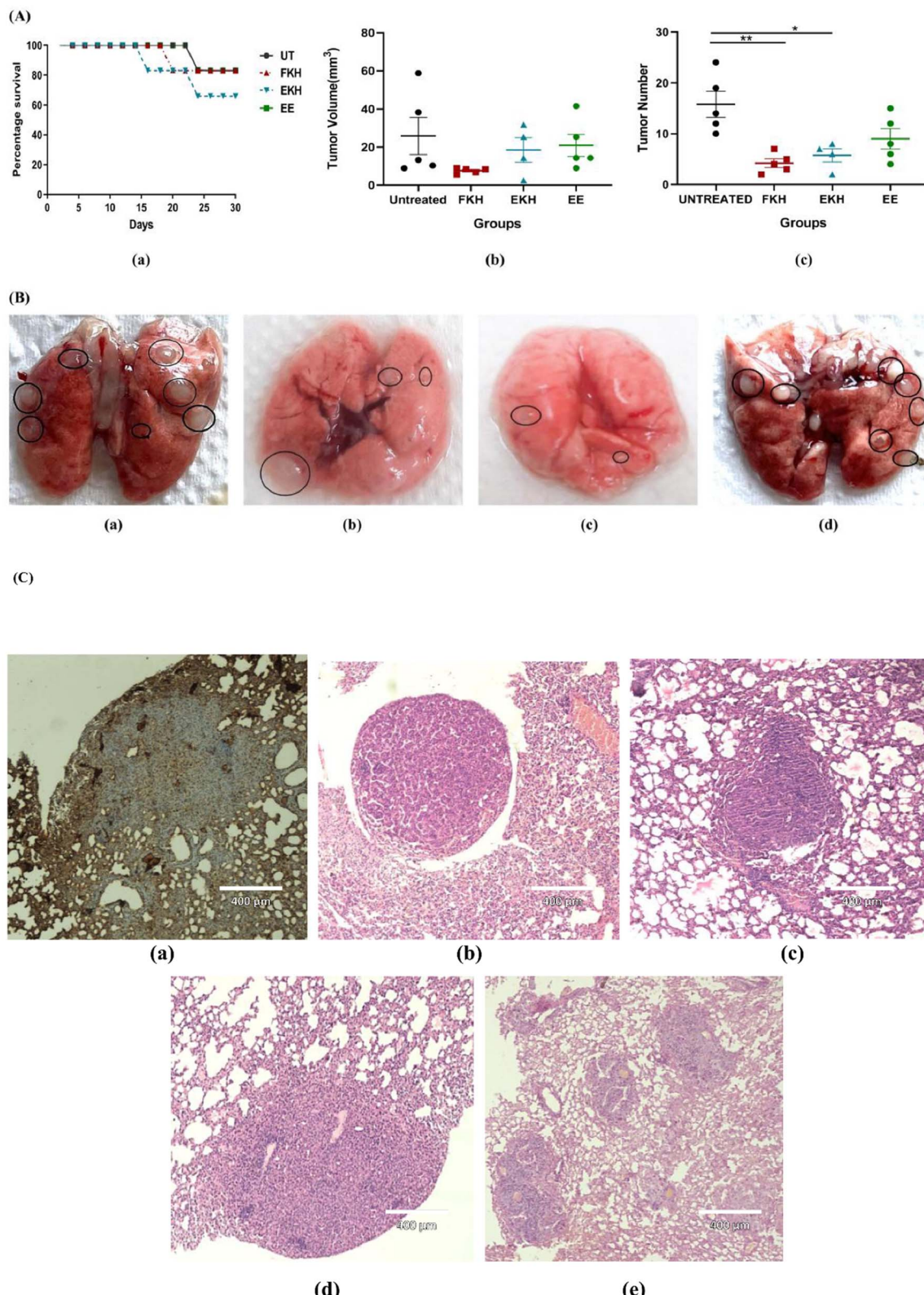


**Fig. 4** *In vivo* antitumor evaluation. (A) Survival analysis and lung tumor burden estimation: (a) survival chart, (b) tumor volume, and (c) tumor number. (B) Representative tumor lesions of (a) untreated group, (b) free potassium hydroxycitrate-treated group, (c) exoformulated potassium hydroxycitrate-treated group, and (d) empty exosome-treated group. (C) Histological images of tumor tissues: (a) TTF-1<sup>+</sup> lung tumor lesions, (b) untreated group, (c) free potassium hydroxycitrate-treated group, (d) exoformulated potassium hydroxycitrate-treated group, and (e) empty exosome-treated group. UT-untreated, FKH-free potassium hydroxycitrate, EKH-exoformulated potassium hydroxycitrate. Black circles depict the tumor lesions. Values are mean  $\pm$  S.E.M of 4–5 animals; \* $P$  < 0.05; \*\* $P$  < 0.01, and \*\*\* $P$  < 0.001.

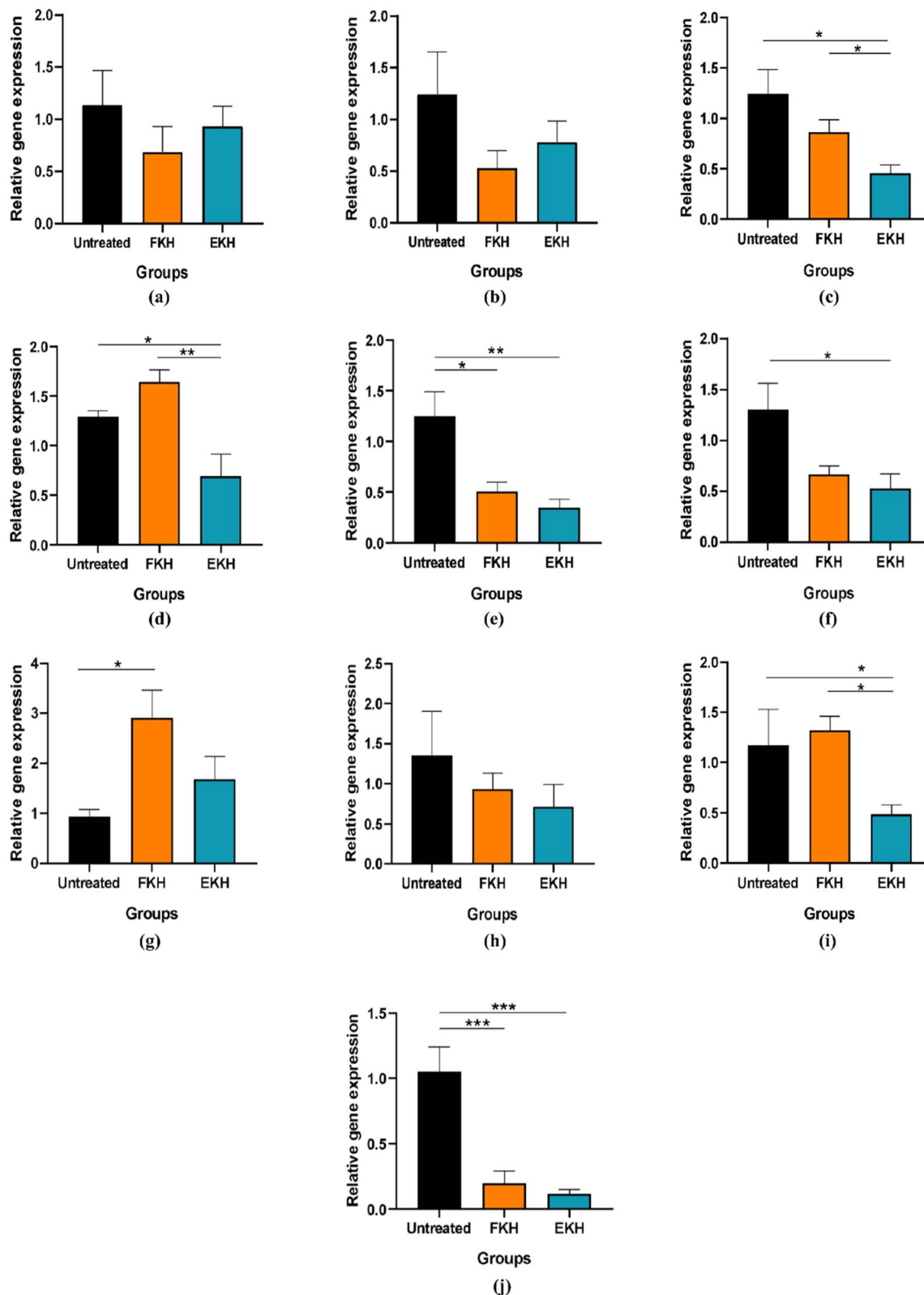


**Fig. 5** mRNA levels of target genes in free potassium hydroxycitrate (FKH) and exoformulation-treated groups (EKH): (a) Epidermal growth factor receptor (EGFR), (b) folate receptor  $\alpha$  (FR  $\alpha$ ), (c) ATP citrate lyase (ACLY), (d) fatty acid synthase (FASN), (e) acetyl CoA carboxylase (ACC), (f) HMG-CoA reductase (HMGCR), (g) citrate synthase (CS), (h) isocitrate dehydrogenase 1 (ICD1), (i) sterol element regulatory binding protein 1c (SERBP1c) and (j) protein kinase B (AKT). Values are represented as mean  $\pm$  S.E.M. of 4–5 animals; \* $P$  < 0.05; \*\* $P$  < 0.01, and \*\*\* $P$  < 0.001.



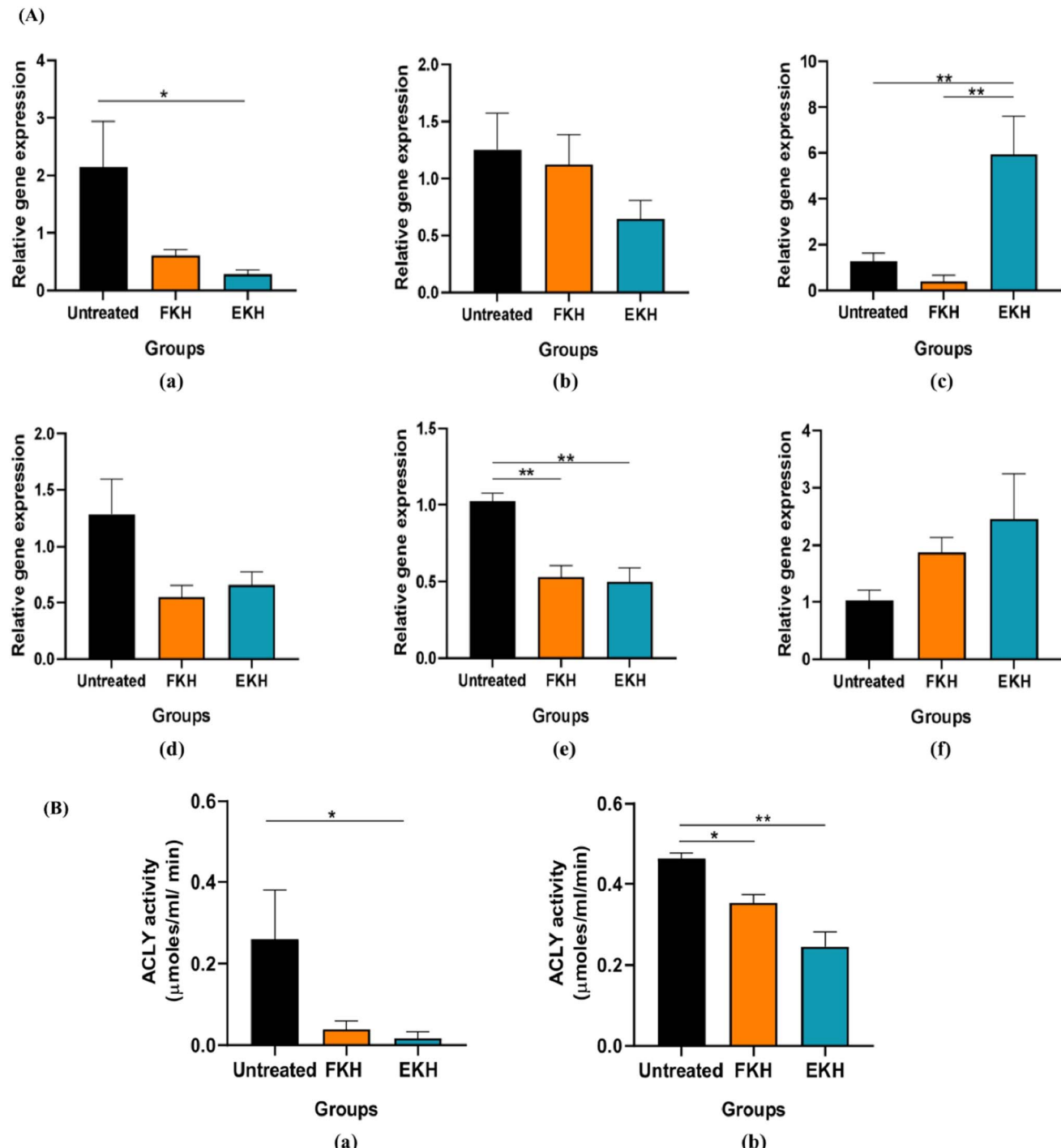


**Fig. 6** (A) mRNA levels of apoptosis- and autophagy-related markers in free potassium hydroxycitrate (FKH)- and exoformulation-treated groups (EKH): (a) B-cell lymphoma 2 (BCL-2), (b) Bcl-2 associated X-protein (BAX), (c) caspase-3, (d) microtubule-associated protein 1A/1B-light chain 3 (LC3B), (e) autophagy-related gene 5 (ATG5) and (f) beclin-1. Values are represented as mean  $\pm$  S.E.M. of 4–5 animals; \* $P$  < 0.05; \*\* $P$  < 0.01, and \*\*\* $P$  < 0.001. (B) ACLY activity in free potassium hydroxycitrate (FKH)- and exoformulation-treated groups (EKH): (a) serum samples and (b) tumor samples. Values are represented as mean  $\pm$  S.E.M. of 4–5 animals; \* $P$  < 0.05; \*\* $P$  < 0.01, and \*\*\* $P$  < 0.001.

Exosomes are small vesicles 30–150 nm in size and are secreted by various cell types such as natural killer cells,<sup>34</sup> brain neuronal U87 cells<sup>34</sup> and macrophages.<sup>21</sup> They are present in all body fluids such as blood, milk, saliva, and urine.<sup>35,36</sup> Exosome based drug delivery systems are preferred over other drug carriers due to their biocompatibility, immunologically

inertness and ability to reach the target efficiently. Human and bovine milk contain various immune-regulatory miRNAs and mRNAs that are involved in maintaining immune tolerance by controlling regulatory T (Treg) cell development.<sup>37</sup> Colostrum also contains several miRNAs that regulate genes related to mammary gland function and are responsible for its greater

immune-boosting effects compared with matured milk.<sup>38</sup> Studies have evaluated the safety and potential side effects of exosome loaded drugs to determine their therapeutic value in the clinical setting and it has been observed that these exosome-based formulations do not cause any toxicity.<sup>20–22</sup> It was observed that, when ExoPAC was administered orally, the relative size of spleen and proportions of cells, number of B cells and neutrophils, in the bone marrow were not altered. These studies suggest that ExoPAC does not have major toxic effects on the immune system, while PAC slightly disturbs the immune system.<sup>26</sup> Similarly, celastrol-loaded exosomes administered to wild-type C57BL6 mice did not cause any gross or systemic toxicity. The exformulation enhances the efficacy of celastrol, thereby reducing the dose related toxicity.<sup>39</sup>

In the present study, bovine milk was used because it is an abundant, safe, and readily available source of exosomes.<sup>28,40</sup> The conjugation of folate to the exosomes surface will make the exosome formulation more targeted towards the cancer cells as the folate receptor alpha is abundantly present on the cancer cells. These vesicles have shown great potential in treatment of severe disorders like cancer, Parkinson's disease, etc.<sup>41,42</sup> We loaded potassium hydroxycitrate into the exosomes to improve its bioavailability and anti-cancer potential.

Exosomes isolated from the bovine milk loaded with potassium hydroxycitrate were in the nanometre range and had spherical morphology. The encapsulation efficiency of KH was approximately 18% and folate conjugation was performed on the exosome surface to improve the targeting ability of this exoformulation. Pharmacokinetic studies revealed that the exosomal formulation exhibited a sustained release profile as evident from the low clearance value and high  $T_{1/2}$  in healthy balb/c mice (Table 2) and Exo KH showed higher drug levels in the lung, spleen, and kidney, depicting the enhanced bioavailability of this exoformulation. Moreover, the exoformulation had improved therapeutic outcomes in terms of reduction in tumor growth and ACLY expression. Thus, the exosomes encapsulating potassium hydroxycitrate depicted significantly higher inhibition of the metabolic enzymes ACLY, FASN, ACC, HMGCR, and ICD1 compared with its free form in a murine model of lung adenocarcinoma.

Earlier studies depicted that hydroxycitrate inhibits ACLY, thereby inducing autophagy.<sup>43,44</sup> In this study, the expression of LC3B and autophagy-related protein 5 was downregulated, whereas beclin-1 expression was upregulated in both free and exoformulation-treated groups compared with the untreated group. Furthermore, ACLY activity decreased significantly in serum and tumor samples of both free and exoformulation-treated groups compared with the untreated group. These observations demonstrate comparable effects of free potassium hydroxycitrate and its exoformulation on ATP citrate lyase activity.

Although exosomes have been widely explored as natural drug delivery vehicles, there are few challenges that need to be addressed before their implementation in the clinical setting, such as inefficient isolation and purification methods, large scale production of exosomes and the identification of its specific biomarkers.<sup>45</sup> Exosome separation and purification

techniques need to be improved to investigate the cargo contents and functions, which will provide insight into their biogenesis. Moreover, this information will be helpful in manipulating the composition of exosomes and study cell interactions, thereby enhancing their therapeutic value. Milk exosomes have clearly demonstrated their potential as drug delivery vehicles. Thus, the development of efficient and robust isolation protocols is required to further explore their translational potential.

## Conclusions

In this study, we demonstrated that raw bovine milk serves as an abundant source for isolating bulk amounts of exosomes and these exosomes have great potential as drug delivery vehicles for both hydrophilic and hydrophobic agents. These natural nanoparticles are able to overcome the poor bioavailability of chemotherapeutic drugs, thereby lowering the total dose and reducing their toxicity. This study was focused on developing an exosomal formulation of potassium hydroxycitrate (Exo-KH) and the anti-cancer potential of this formulation was evaluated *in vivo* against the lung adenocarcinoma mouse model. Cumulatively, the study findings indicated that the encapsulation of hydroxycitrate in folate conjugated exosomes enhanced the anti-proliferative activity of this compound thereby elevating its therapeutic efficacy. To the best of our knowledge this is the first study in which hydroxycitrate has been encapsulated in folate conjugated exosomes, which indicated the possibility of using this formulation against lung cancer.

## Abbreviations

RT-PCR	real time polymerase chain reaction
FASN	fatty acid synthase
ACC	acetyl CoA carboxylase
HMGCR	hydroxy methyl glutaryl CoA reductase
CS	citrate synthase
ICD1	isocitrate dehydrogenase 1
GAPDH	glyceraldehyde-3-phosphate dehydrogenase
SERBP	sterol element regulatory binding protein
AKT	protein kinase B
TTF-1	thyroid transcription factor 1
ctDNA	circulating tumor DNA
cDNA	complementary DNA
TBS	tris buffered saline

## Data availability

The authors confirm that the data supporting the findings of this study are available within the article.

## Author contributions

All authors have given final approval for the publication of the manuscript. Kanika Phutela: methodology, data curation,



formal analysis, conceptualization, investigation, writing – original draft, review and editing. Dr Amanjit Bal: investigation. Dr Navneet Singh: investigation. Dr Sadhna Sharma: conceptualization, funding acquisition, supervision.

## Conflicts of interest

The authors report no competing interests in this work.

## Acknowledgements

We are grateful to Department of Science and Technology (DST-INSPIRE division), New Delhi for providing fellowship to Kanika Phutela.

## References

- 1 C. E. Meacham and S. J. Morrison, Tumour heterogeneity and cancer cell plasticity, *Nature*, 2013, **501**(7467), 328–337.
- 2 R. J. Cersosimo, Lung cancer: a review, *Am. J. Health-Syst. Pharm.*, 2002, **59**(7), 611–642.
- 3 C. Zappa and S. A. Mousa, Non-small cell lung cancer: current treatment and future advances, *Transl. Lung Cancer Res.*, 2016, **5**(3), 288–300.
- 4 O. Warburg, On the origin of cancer cells, *Science*, 1956, **123**(3191), 309–314.
- 5 T. Sun, K. Hayakawa, K. S. Bateman and M. E. Fraser, Identification of the citrate-binding site of human ATP-citrate lyase using X-ray crystallography, *J. Biol. Chem.*, 2010, **285**(35), 27418–27428.
- 6 T. Migita, T. Narita, K. Nomura, E. Miyagi, F. Inazuka, M. Matsuura, M. Ushijima, T. Mashima, H. Seimiya, Y. Satoh, S. Okumura, K. Nakagawa and Y. Ishikawa, ATP citrate lyase: activation and therapeutic implications in non-small cell lung cancer, *Cancer Res.*, 2008, **68**(20), 8547–8554.
- 7 H. F. Yancy, J. A. Mason, S. Peters, C. Thompson, G. K. Littleton, M. Jett and A. A. Day, Metastatic progression and gene expression between breast cancer cell lines from African American and Caucasian women, *J. Carcinog.*, 2007, **6**, 8.
- 8 J. Turyn, B. Schlichtholz, A. Dettlaff-Pokora, M. Presler, E. Goyke, M. Matuszewski, Z. Kmiec, K. Krajka and J. Swierczynski, Increased activity of glycerol 3-phosphate dehydrogenase and other lipogenic enzymes in human bladder cancer, *Horm. Metab. Res.*, 2003, **35**(10), 565–569.
- 9 A. Varis, M. Wolf, O. Monni, M. L. Vakkari, A. Kokkola, C. Moskaluk, H. Jr Frierson, S. M. Powell, S. Knuutila, A. Kallioniemi and W. El-Rifai, Targets of gene amplification and overexpression at 17q in gastric cancer, *Cancer Res.*, 2002, **62**(9), 2625–2629.
- 10 G. Hatzivassiliou, F. Zhao, D. E. Bauer, C. Andreadis, A. N. Shaw, D. Dhanak, S. R. Hingorani, D. A. Tuveson and C. B. Thompson, ATP citrate lyase inhibition can suppress tumor cell growth, *Cancer Cell*, 2005, **8**(4), 311–321.
- 11 T. A. Berkhouit, L. M. Havekes, N. J. Pearce and P. H. Groot, The effect of (-)-hydroxycitrate on the activity of the low-density-lipoprotein receptor and 3-hydroxy-3-methylglutaryl-CoA reductase levels in the human hepatoma cell line Hep G2, *Biochem. J.*, 1990, **272**(1), 181–186.
- 12 L. Schwartz, M. Abolhassani, A. Guais, E. Sanders, J. M. Steyaert, F. Campion and M. Israël, A combination of alpha lipoic acid and calcium hydroxycitrate is efficient against mouse cancer models: preliminary results, *Oncol. Rep.*, 2010, **23**(5), 1407–1416.
- 13 B. S. Jena, G. K. Jayaprakasha, R. P. Singh and K. K. Sakariah, Chemistry and biochemistry of (-)-hydroxycitric acid from *Garcinia*, *J. Agric. Food Chem.*, 2002, **50**(1), 10–22.
- 14 K. L. Zambell, M. D. Fitch and S. E. Fleming, Acetate, and butyrate are the major substrates for de novo lipogenesis in rat colonic epithelial cells, *J. Nutr.*, 2003, **133**(11), 3509–3515.
- 15 P. E. Feuser, L. D. S. Bubniak, M. C. D. S. Silva, A. D. C. Viegas, A. C. Fernandes, E. Ricci-Junior, M. Nele, A. C. Tedesco, C. Sayer and P. H. H. de Araújo, Encapsulation of magnetic nanoparticles in poly(methyl methacrylate) by miniemulsion and evaluation of hyperthermia in U87MG cells, *Eur. Polym. J.*, 2015, **68**, 355–365.
- 16 K. Greenhalgh and E. Turos, In vivo studies of polyacrylate nanoparticle emulsions for topical and systemic applications, *Nanomed. Nanotechnol. Biol. Med.*, 2009, **5**(1), 46–54.
- 17 Z. Zhang, P. C. Tsai, T. Ramezanli and B. B. Michniak-Kohn, Polymeric nanoparticles-based topical delivery systems for the treatment of dermatological diseases, *Wiley Interdiscip. Rev.: Nanomed. Nanobiotechnol.*, 2013, **5**(3), 205–218.
- 18 S. Dasgupta, T. Auth and G. Gompper, Shape and orientation matter for the cellular uptake of nonspherical particles, *Nano Lett.*, 2014, **14**(2), 687–693.
- 19 J. Qin and Q. Xu, Functions and application of exosomes, *Acta Pol. Pharm.*, 2014, **71**(4), 537–543.
- 20 Y. Tian, S. Li, J. Song, T. Ji, M. Zhu, G. J. Anderson, J. Wei and G. Nie, A doxorubicin delivery platform using engineered natural membrane vesicle exosomes for targeted tumor therapy, *Biomaterials*, 2014, **35**(7), 2383–2390.
- 21 M. S. Kim, M. J. Haney, Y. Zhao, V. Mahajan, I. Deygen, N. L. Klyachko, E. Inskoe, A. Piroyan, M. Sokolsky, O. Okolie, S. D. Hingtgen, A. V. Kabanov and E. V. Batrakova, Development of exosome-encapsulated paclitaxel to overcome MDR in cancer cells, *Nanomedicine*, 2016, **12**(3), 655–664.
- 22 V. H. Ferreira, A. Nazli, S. E. Dizzell, K. Mueller and C. Kaushic, The anti-inflammatory activity of curcumin protects the genital mucosal epithelial barrier from disruption and blocks replication of HIV-1 and HSV-2, *PLoS One*, 2015, **10**(4), e0124903.
- 23 J. Boorn, M. Schlee, C. Coch and G. Hartmann, siRNA delivery with exosome nanoparticles, *Nat. Biotechnol.*, 2011, **29**, 325–326.
- 24 M. Vashisht, P. Rani, S. K. Onteru and D. Singh, Curcumin Encapsulated in Milk Exosomes Resists Human Digestion



and Possesses Enhanced Intestinal Permeability in Vitro, *Appl. Biochem. Biotechnol.*, 2017, **183**(3), 993–1007.

25 W. E. Bawarski, E. Chidlowsky, D. J. Bharali and S. A. Mousa, Emerging nanopharmaceuticals, *Nanomedicine*, 2008, **4**, 273–282.

26 A. K. Agrawal, *et al.*, Milk-derived exosomes for oral delivery of paclitaxel, *Nanomedicine*, 2017, 1–10.

27 O. Young, N. Ngo, L. Lin, L. Stanbery, J. F. Creeden, D. Hamouda and J. Nemunaitis, Folate Receptor as a Biomarker and Therapeutic Target in Solid Tumors, *Curr. Probl. Cancer*, 2023, **47**(1), 100917.

28 R. Munagala, F. Aqil, J. Jeyabalan and R. C. Gupta, Bovine milk-derived exosomes for drug delivery, *Cancer Lett.*, 2016, **371**(1), 48–61.

29 P. Ahlawat, K. Phutela, A. Bal, N. Singh and S. Sharma, Therapeutic potential of human serum albumin nanoparticles encapsulated actinonin in murine model of lung adenocarcinoma, *Drug Delivery*, 2022, **29**(1), 2403–2413.

30 H. M. Abdelaziz, A. O. Elzoghby, M. W. Helmy, M. W. Samaha, J. Y. Fang and M. S. Freag, Liquid crystalline assembly for potential combinatorial chemo-herbal drug delivery to lung cancer cells, *Int. J. Nanomed.*, 2019, **14**, 499–517.

31 O. Fiala, P. Hosek, M. Pesek, *et al.*, Serum concentration of erlotinib and its correlation with outcome and toxicity in patients with advanced-stage NSCLC, *Anticancer Res.*, 2017, **37**, 6469–6476.

32 A. Ismail, A. S. Doghish, M. E. B. Elsadek, S. A. Salama and A. D. Mariee, Hydroxycitric acid potentiates the cytotoxic effect of tamoxifen in MCF-7 breast cancer cells through inhibition of ATP citrate lyase, *Steroids*, 2020, **160**, 108656.

33 M. Logozzi, A. De Milito, L. Lugini, M. Borghi, L. Calabro, M. Spada, M. Perdicchio, M. L. Marino, C. Federici, E. Iessi, D. Brambilla, G. Venturi, F. Lozupone, M. Santinami, V. Huber, M. Maio, L. Rivoltini and S. Fais, High levels of exosomes expressing CD63 and caveolin-1 in plasma of melanoma patients, *PLoS One*, 2009, **4**(4), 5219.

34 D. Han, K. Wang, T. Zhang, G. C. Gao and H. Xu, Natural killer cell-derived exosome-entrapped paclitaxel can enhance its anti-tumor effect, *Eur. Rev. Med. Pharmacol. Sci.*, 2020, **24**(10), 5703–5713.

35 M. Simons and G. Raposo, Exosomes-vesicular carriers for intercellular communication, *Curr. Opin. Cell Biol.*, 2009, **21**(4), 575–581.

36 B. Li, A. Hock, R. Y. Wu, A. Minich, S. R. Botts, C. Lee, L. Antounians, H. Miyake, Y. Koike, Y. Chen, A. Zani, P. M. Sherman and A. Pierro, Bovine milk-derived exosomes enhance goblet cell activity and prevent the development of experimental necrotizing enterocolitis, *PLoS One*, 2019, **14**(1), e0211431.

37 J. Qin and Q. Xu, Functions and application of exosomes, *Acta Pol. Pharm.*, 2014, **71**(4), 537–543.

38 S. M. Davidson, K. Takov and D. M. Yellon, Exosomes and Cardiovascular Protection, *Cardiovasc. Drugs Ther.*, 2017, **31**(1), 77–86.

39 T. Kouwaki, Y. Fukushima, T. Daito, T. Sanada, N. Yamamoto, E. J. Mifsud, C. R. Leong, K. Tsukiyama-Kohara, M. Kohara, M. Matsumoto, T. Seya and H. Oshiumi, Extracellular Vesicles Including Exosomes Regulate Innate Immune Responses to Hepatitis B Virus Infection, *Front. Immunol.*, 2016, **7**, 335.

40 G. Mariño, F. Pietrocola, T. Eisenberg, Y. Kong, S. A. Malik, A. Andryushkova, S. Schroeder, T. Pendl, A. Harger, M. Niso-Santano, N. Zamzami, M. Scoazec, S. Durand, D. P. Enot, Á. F. Fernández, I. Martins, O. Kepp, L. Senovilla, C. Bauvy, E. Morselli, E. Vacchelli, M. Bennetzen, C. Magnes, F. Sinner, T. Pieber, C. López-Otín, M. C. Maiuri, P. Codogno, J. S. Andersen, J. A. Hill, F. Madeo and G. Kroemer, Regulation of autophagy by cytosolic acetyl-coenzyme A, *Mol. Cell*, 2014, **53**(5), 710–725.

41 N. Kosaka, H. Izumi, K. Sekine and T. Ochiya, microRNA as a new immune-regulatory agent in breast milk, *Silence*, 2010, **1**, 7.

42 C. Admyre, S. M. Johansson, K. R. Qazi, J. J. Filen, R. Lahesmaa, M. Norman, E. P. Neve, A. Scheynius and S. Gabrielsson, Exosomes with immune modulatory features are present in human breast milk, *J. Immunol.*, 2007, **179**, 1969–1978.

43 F. Aqil, H. Kausar, A. Kumar Agrawal, J. Jeyabalan, Al-H. Kyakulaga, R. Munagala and R. Gupta, Exosomal formulation enhances therapeutic response of celastrol against lung cancer, *Exp. Mol. Pathol.*, 2016, **101**(1), 12–21.

44 F. Pietrocola, J. Pol, E. Vacchelli, S. Rao, D. P. Enot, E. E. Baracco, S. Levesque, F. Castoldi, N. Jacquemet, T. Yamazaki, L. Senovilla, G. Marino, F. Aranda, S. Durand, V. Sica, A. Chery, S. Lachkar, V. Sigl, N. Bloy, A. Buque, S. Falzoni, B. Ryffel, L. Apetoh, F. Di Virgilio, F. Madeo, M. C. Maiuri, L. Zitvogel, B. Levine, J. M. Penninger and G. Kroemer, Caloric Restriction Mimetics Enhance Anticancer Immunosurveillance, *Cancer Cell*, 2016, **30**(1), 147–160.

45 X. Li, A. L. Corbett, E. Taatizadeh, N. Tasnim, J. P. Little, C. Garnis, M. Daugaard, E. Guns, M. Hoofar and I. T. S. Li, Challenges and opportunities in exosome research-Perspectives from biology, engineering, and cancer therapy, *APL Bioeng.*, 2019, **3**(1), 011503.

